



# Mechanism of Reducing Local Flow Velocity Using Obstacle Trenches in Microfluidics

Teeraphat Kongsaktrakul<sup>1</sup>, Alongkorn Pimpin<sup>1</sup>, Ampol Kamnerdsook<sup>2</sup> and Thammawit Suwannaphan<sup>2,3\*</sup>

<sup>1</sup> Department of Mechanical Engineering, Faculty of Engineering, Chulalongkorn University, Bangkok

<sup>2</sup> Department of Mechanical Engineering Technology, College of Industrial Technology (CIT), King Mongkut's University of Technology North Bangkok, Bangkok

<sup>3</sup> Center of Sustainable and Energy Engineering Materials, Department of Mechanical Engineering Technology, College of Industrial Technology, King Mongkut's University of Technology North Bangkok

\* Corresponding author, E-mail: thammawit.s@cit.kmutnb.ac.th

Received: 1 October 2024; Revised: 15 January 2025; Accepted: 27 January 2025

Online Published: 22 April 2025

**Abstract:** Trapping efficiency in microwell technique is influenced by both microwell geometry and flow velocity. At higher flow velocity, microplastics tend to flow over microwells resulting in reduced trapping efficiency. Therefore, decreasing flow velocity to enhance trapping efficiency is important. This research introduces triangular obstacle trenches in front of the microwells to reduce local flow velocity leading to the improvement of trapping efficiency. The simulation results show that two mechanisms must occur concurrently to effectively reduce local flow velocity. They are the spreading of streamlines from the apex to the back of triangular trench, and the suitable recirculation inside the trench. In this study, the obstacle trench has dimensions of 600  $\mu\text{m}$  on each side with a depth of 300  $\mu\text{m}$  while the square microwell measured 1,000  $\mu\text{m}$  on each side with a depth of 600  $\mu\text{m}$ . The flow rate was at 0.3 ml/min. Experiments confirmed that the use of triangular obstacle trenches significantly enhanced trapping efficiency by 30 times compared to the case without trenches.

**Keywords:** Microfluidics; Microplastics; Obstacle trenches; Trapping; Microwells



## 1. Introduction

Microplastic contamination has been drawn a great concern as a serious global issue with tiny particles entering water supplies and human tissue. Recently, microplastics were found within bodies of human [1-2]. This finding sparked concerns about the potential harmful effects of microplastics to human health. In addition, microplastics can absorb [3], and carry toxic contaminants [4]. These toxic substances enter and then diffuse toxicities into living human's body resulting in detrimental effects on human health including nausea, irritation, diarrhea, vomiting and confusion [5]. Human may accidentally consume microplastics through food or water, and these particles can be found in bottled water, inhalation and dermal contact, especially from water sources [6]. For this, raising public awareness of microplastic contamination by detecting microplastics in water bodies is significantly important to quality of human's life and environments.

A number of techniques have been developed for microplastic detection, especially, for identifying small amount of microplastics within large sample volumes. These methods often demand interdisciplinary across various fields such as engineering, chemistry, biology and environment science as well as access to advanced equipment, specialized facilities and well-equipped laboratories. To address these challenges, microfluidic techniques

have drawn significant interest in microplastic detection. Due to their versatility, microfluidic technologies have shown significant promise and growth, especially in water quality monitoring.

Trapping techniques are commonly used to capture small particles in large sample volumes for analysis through a light microscope. Among various techniques [7-11], microwell trapping technique [12] shows a great potential for trapping particles without the need for external forces. Moreover, it allows for the real-time detection of small amounts of microplastics in large sample volumes.

The principles of microwell trapping rely on the balance between two forces—gravitational force and hydrodynamic force. When the gravitational force is stronger than the hydrodynamic force, the particles are effectively dragged and trapped in microwells regardless of their shape. In contrast, when the hydrodynamic force is stronger than the gravitational force, particles are dragged out or floated over the microwells, reducing trapping efficiency [13-14].

In real-world application, a microwell trapping device can be directly installed in a water pipe to capture debris and contaminants, particularly microplastics from tap water. However, a high flow rate in a water pipe may possibly result in reducing trapping efficiency due to the strong of the hydrodynamic force as previously mentioned. To address this issue, it is important to reduce flow velocity locally in front of the microwells. Previously,



the technique to reduce flow velocity across the entire cross-section is preferred. However, it is not practical such as microplastics may stick on a pipe's surface. Moreover, the hydrodynamic force exerting on particles should be small before moving forward the microwell in order to enhance the possibility of trapping. Thus, a new method of reducing local flow velocity in front of the trapping microwells for improving microplastic trapping efficiency is proposed.

According to our previous studies, we proposed the use of array of triangle microwells for particle trapping. We observed that the microwells in the first row were unable to trap particles well while the second row successfully trapped most particles that passed through. This observation led us to explore how the first row of microwells influences the trapping efficiency of the second row. We believed that a local flow velocity reduction from the first-row of microwells responds to the increasing of trapping efficiency.

In this study, the triangular obstacle trenches are introduced in front of the microwells to reduce local flow velocity before microplastics are trapped. The principle behind the obstacle trenches is that as microplastics flow along the fluid flow stream and approach the obstacle trenches, they tend to be dragged into the trenches due to recirculation within the trenches. Once flowing into the trench, microplastics are eventually dragged out of the trenches. In this stage, as microplastics are dragged

out of the trenches to the surface, microplastics tend to move slowly and roll on the surface at a lower speed. This slower movement allows them to be trapped easily in the next-row (microwells) as shown in Fig. 1. In addition, the trench will not introduce flow resistance as much as the other structures penetrating into the main flow.

The purpose of this research is to investigate the mechanism of obstacle trenches that reduces local flow velocity, and analyze key parameters that potentially effect the reduction in local flow velocity. The research also serves guideline for alternative trench designs to further reduce local flow velocity for enhancing the trapping efficiency.

## 2. Systematic concept

Based on our previous findings [13-14], we hypothesized that microplastics were dragged into the trench resulting in reducing both flow velocity and the distance from the surface as shown in Fig. 1.

In this research, an engineering program (COMSOL Multiphysics) is used to investigate the mechanism and key parameters that influence the reduction of local flow velocity. The governing equations for fluid flow in this model are derived from the Navier-Stokes equations, expressed as:

$$\rho(\partial u/\partial t) + \rho(u \cdot \nabla)u = -\nabla p + \mu \nabla^2 u$$

Here,  $\rho$  is the fluid density ( $998 \text{ kg/m}^3$ ),  $\mu$  is the dynamic viscosity ( $0.001 \text{ Pa}\cdot\text{s}$ ),  $u$  is the velocity field, and  $p$  is the pressure field. The fluid



flow behaves as Newtonian and is defined as laminar and incompressible. No slip condition is applied to the walls. The inlet's entrance is set to be fully developed at 0.3 ml/min while the outlet allows for no suppress backflow (Fig. 2).

To explore the effects of trench design on these parameters, three models of obstacle trenches—triangle, square and circle shape are simulated to investigate the effects on velocity and streamline after passing from them. We found that the triangular trench allowed only streamlines toward the apex moving into it. This

would result in trapping of a smaller number of particles in the trench as showed in Fig. 3. Interestingly, the streamlines at the back also tended to move closer to the surface. For other designs including square and circular trenches, the streamlines at the front and the back remained the same distance from the surface with a large area of recirculation inside. Among these designs, the square trench provided the large recirculation. Consequently, it increased the higher possibility for trapping a larger number of microplastics.

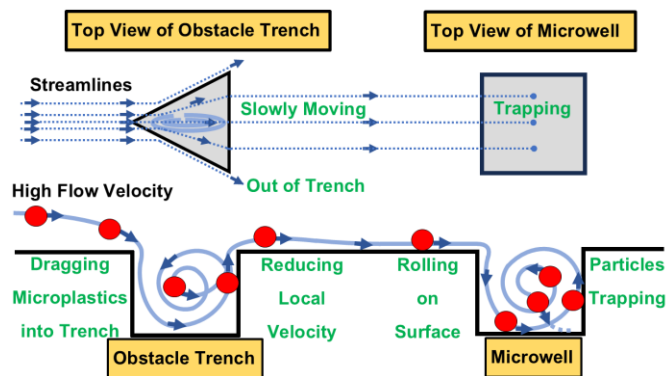


Fig. 1 Working principles of obstacle trench and microwells to enhance particle trapping inside the microwells

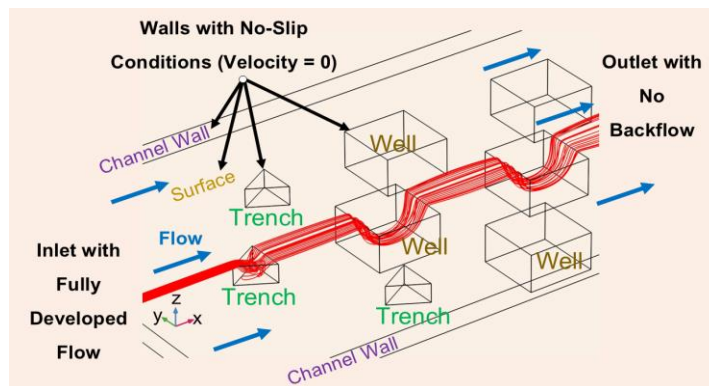
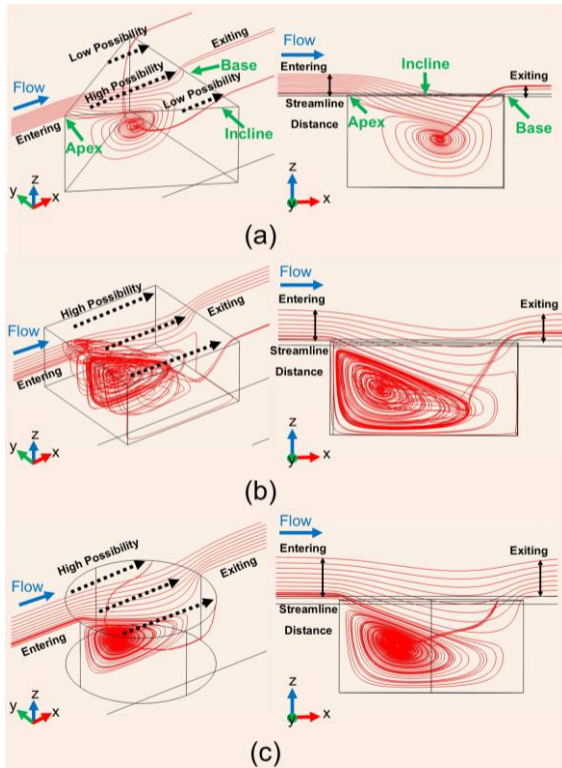


Fig. 2 Boundary condition setup for the model



**Fig. 3** Various designs of a trench showing the possibility for trapping and the distance of streamlines entering and exiting the trench  
(a) triangle (b) square and (c) circle

Based on the ability to reduce flow velocity, lower the distance of streamlines from the surface and create small recirculation inside, the triangular trench is chosen. Meanwhile, for the microwell, the square shape is chosen due to the large recirculation so that it has high possibility of particle trapping.

### 3. Proposed mechanism

We examined flow velocity and recirculation patterns in a 3D model through the equilateral triangular obstacle trench and square microwell. To ensure the accuracy of the flow velocity results, a mesh independence analysis was conducted by progressively refining the mesh until the flow velocity results reached stability. The mesh density on the obstacle trenches and microwells are customized with maximum and minimum element size of 30 and 0.3  $\mu\text{m}$  with the total meshes of approximately  $3 \times 10^6$  elements in this model.

We discovered that there were two important mechanisms that must occur concurrently to let streamlines into the obstacle trenches. The first thing was only the streamlines moving toward at the apex of triangular obstacle trench is allowed to move inside. Other streamlines that moved toward the inclined lines of triangle would not go into the trench. This is a unique flow pattern for a triangular trench [13-14].

Secondly, the streamlines moving toward the apex were recirculated whose strength was depended on the shape and depth of trench. If the trenches are too shallow, the recirculation will not occur. Therefore, the microplastics that are suspended in the flow will not being trapped but dragged out from the trenches (Fig. 4(a)). However, if the trenches are too deep, most microplastics will be trapped within the trenches instead (Fig. 4(c-d)).



For this, the depth of the triangular obstacle trenches should be deep enough to create sufficient recirculation to reduce local flow velocity instead of trapping microplastics. Therefore, the depth of trench is one of the crucial factors that can influence either reducing local flow velocity or trapping particles.

#### A. Depth and flow recirculation

To determine the appropriate depth, triangular trench of 600  $\mu\text{m}$  in each side with four different trench depths were examined. The results showed that increasing the trench depth, the recirculation became larger. However, increasing depth beyond a certain depth, it had no effect on recirculation. Therefore, the trench depth should remain shallower than the critical depth.

According to the simulation, we found that the trench depth of shallower than about 300  $\mu\text{m}$  did not generate recirculation (Fig. 4(a)) while a depth of about 300  $\mu\text{m}$  was sufficient to induce strong recirculation (Fig. 4(b)). As the depth increased beyond 300  $\mu\text{m}$ , recirculation became larger until it reached to 600  $\mu\text{m}$ . At this depth, recirculation extended to the bottom of the trench (Fig. 4(c)). Beyond 600  $\mu\text{m}$  depth, a large area of recirculation occurred but its size remained constant and no longer correlated with trench depth (Fig. 4(d)). Based on these findings, the trench depth was set at 300  $\mu\text{m}$  about the half of the triangular trench side that was set at 600  $\mu\text{m}$ .

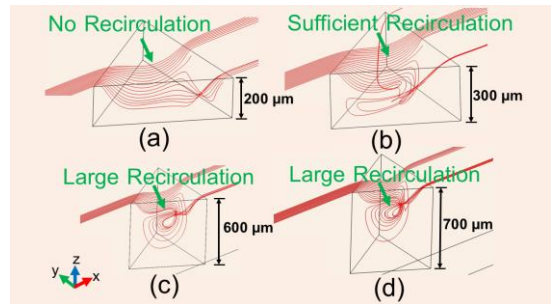


**Fig. 4** Various depth for triangular obstacle trench at (a) 200, (b) 300, (c) 600 and (d) 700  $\mu\text{m}$

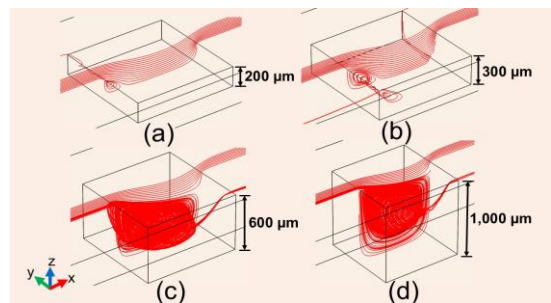


**Fig. 5** Various depth for square microwells at (a) 200, (b) 300, (c) 600 and (d) 1,000  $\mu\text{m}$

Using same concept, a 1,000  $\mu\text{m}$  square microwell with varying depths was simulated to study recirculation. At a depth of 200  $\mu\text{m}$ , a small recirculation formed at the front of square microwell (Fig. 5(a)) and gradually increased as the microwell depth increased (Fig. 5(b)).

At a depth of 600  $\mu\text{m}$ , streamlines became fully recirculated within the microwells (Fig. 5(c)). This suggests that the depth of 600  $\mu\text{m}$  was the critical value for particle trapping, as it is equivalent to approximately the half of the length of the microwell's side. Once the depth surpassed



600  $\mu\text{m}$ , the recirculation pattern remained unchanged, however, the recirculation zone continued to extend as the microwell depth increased (Fig. 5(d)).

#### B. Distance of streamlines from a surface

Furthermore, we analyzed the distance of the streamlines from the surface at the front and the back of the trench. The distance of streamlines entering the trench was determined by plotting streamlines at the center of the trench (apex) on the x-z plane. It was discovered that the streamlines were separated into three distinct distance regions. In the first region, streamlines were recirculated into the trench. In the second region, streamlines entered the trench but did not recirculate. However, in the third region and above, streamlines flowed over the trench as shown in Figs. 6.

To measure the distance and velocity of the streamlines at the front and the back of the trench, the farthest distance of the streamline from the bottom surface and its velocity magnitude in each region was measured. The results of the 1<sup>st</sup> region (Fig.6 (a)), showed that the distance entering the trench was approximately 45  $\mu\text{m}$  at velocity of 2 mm/s. At the exit, the level of the streamline was reduced to approximately 20  $\mu\text{m}$  at a velocity of about 1 mm/s. This suggests that the distance of the streamlines and the local velocity were about half decreased. At the back, most streamlines in the

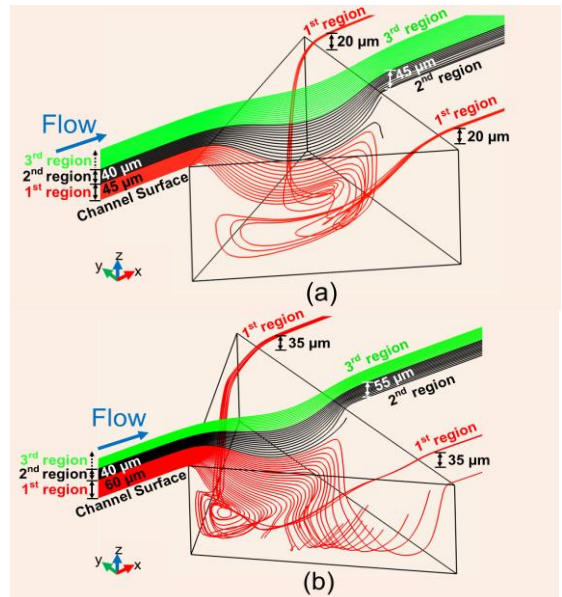


**Fig. 6** Streamlines in three regions flowing toward (a) an equilateral and (b) right-angle triangular trench

1<sup>st</sup> region spread out from the apex to the corners of the triangular base.

In the 2<sup>nd</sup> region, most streamlines with the level between 45 to 85  $\mu\text{m}$  from the surface were curved into the trench to the depth of 100  $\mu\text{m}$  and then exited through the middle of the trench at a maximum distance of about 45  $\mu\text{m}$  from the surface without recirculating. In the 3<sup>rd</sup> region, above the level of approximately 85  $\mu\text{m}$  from the surface, all streamlines remained above the trench.

Furthermore, at the level of approximately 45  $\mu\text{m}$  (1<sup>st</sup> region) from the surface, only streamlines within the region about 50  $\mu\text{m}$  around its apex entered the trench. These streamlines expanded to





#### 4. Prototype of obstacles and microwells

To evaluate the efficacy of obstacle trench, an experiment is conducted by introducing triangular obstacle trench in front of square microwells. The number of particles trapped in microwells then is counted to evaluate and compare the effectiveness of trapping.

##### A. Design of the system

The microfluidic system is fabricated using a polymer-casting technique. The microfluidic channel is designed in a chamber with 15 mm in width and 65 mm in length and 600  $\mu\text{m}$  in height as shown in Fig. 8. One reason for extending the chamber's length is to ensure that the fluid flow from the inlet to the outlet is fully developed before reaching obstacle trenches.

The chamber's central region is divided into two sections. The first section is obstacle trenches which are designed in equilateral triangular shape with 600  $\mu\text{m}$  in each side and 300  $\mu\text{m}$  in depth (Fig. 9(a)). In contrast, the second design is a right triangle with a 90° apex angle and 300  $\mu\text{m}$  in depth as demonstrated in Fig. 9(b). The second section is microwells which are designed in a square shape with 1,000  $\mu\text{m}$  in each side and 600  $\mu\text{m}$  in depth as showed in Fig. 9(c).

For the alignment, obstacle trenches and microwells are arranged in a chessboard pattern with six columns and three rows. This pattern is designed to minimize flow disturbance caused by

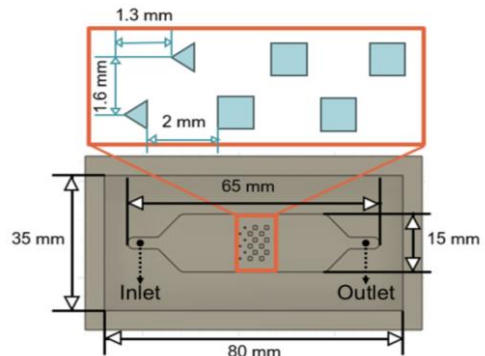


Fig. 8 Dimension of microfluidic device

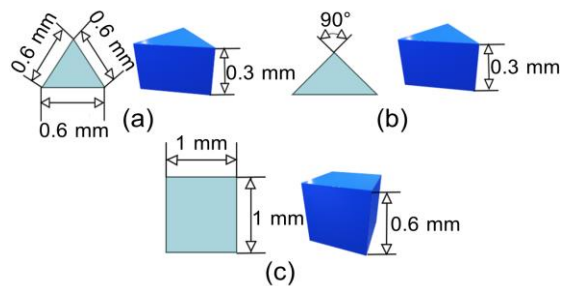


Fig. 9 Dimensions of (a) equilateral triangular trench (b) right-angle triangular trench and (c) square microwell

adjacent trench structures. The first row consists of triangular obstacle trenches while the 2<sup>nd</sup> and 3<sup>rd</sup> rows consist of square microwells. The distance from the apex of an obstacle to another is 1.6 mm while the distance from the base of a triangular obstacle trench to the leading edge of a microwell is 2 mm.

##### B. Fabrication and sample preparation

The mold for polymer casting is fabricated using a 3D resin printing technique. Polydimethylsiloxane (PDMS) are mixed together with a curing agent



(CAT-RG) in a 10:1 ratio. After that, vacuum pump is used to eliminate air bubbles from the mixture. Later, the mixture is carefully poured into the mold and then heated to harden leading to the formation of flow chamber and microwell part.

Both parts are then bonded together using the oxygen plasma to bond the upper part (flow chamber) to the bottom part (microwells) together to enclose these two parts as an assembled device. Finally, the assembled device is connected by microtubes (inlet and outlet). Fig. 10 demonstrates the actual microfluidic device and microplastics are trapped in a microwell.

For sample preparation, polystyrene beads of 10  $\mu\text{m}$  diameter are suspended in deionized (DI) water. Several trials are examined to determine the optimal concentration of beads to achieve low level of uncertainty in experiments. Finally, the concentration was chosen at  $5 \times 10^4$  particles/ml.

## 5. Experimental results

A microplastic suspension was introduced in microfluidic system at 0.3 ml/min for 10 minutes. The number of microplastics was counted using a light microscope and tally counter. To understand the effects of obstacle trenches on the trapping in microwells, three designs of trench models—equilateral, right-angle and no obstacle (control) trenches were examined repeatedly three times.

The system consisted of six obstacle trenches in the 1<sup>st</sup> row followed by six front-microwells in the

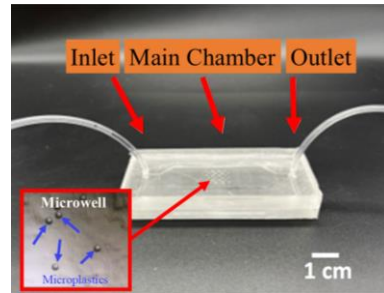


Fig. 10 Microfluidic device and microplastic beads of 10  $\mu\text{m}$  trapped in wells

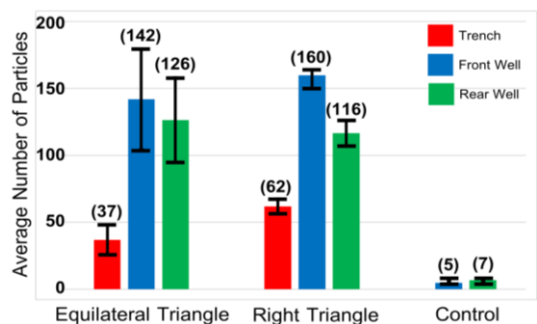


Fig. 11 The average number of microplastics trapped in three experimental cases

2<sup>nd</sup> row and six rear-microwells in the 3<sup>rd</sup> row. The total number of trapped microplastics in each row was counted and averaged to determine the trapping efficiency as shown in Fig.11.

According to the results of equilateral triangle, a small number of microplastics were trapped in the obstacle trenches averaging about  $37 \pm 11$  particles. In contrast, the majority of trapped microplastics were found in the front square microwells (2<sup>nd</sup> row) with an average of  $142 \pm 37$  particles and in the rear square microwells (3<sup>rd</sup> row) with an average of  $126 \pm 32$  particles.



For the right-angle design, most microplastics were trapped in the front microwells (2<sup>nd</sup> row) and rear microwells (3<sup>rd</sup> row) averaging  $160\pm 4$  and  $116\pm 10$  particles, respectively while the obstacle trenches trapped a small number of particles with an average of  $62\pm 6$  particles.

In control case, there was no obstacle trenches introduced in front of the microwells. A small number of microplastics in the front and rear microwells (2<sup>nd</sup> and 3<sup>rd</sup>) were comparably trapped. The number of microplastics in front microwells averaging  $5\pm 1$  particles while the rear microwells averaging  $7\pm 1$  particles were significant lower compared to the equilateral and right-angle trench design.

The results suggest that the amount of trapped microplastics in the microwells with the triangular obstacle trenches was about 30 times higher than in the control case. Furthermore, the right-angle trenches showed slightly higher particle trapping efficiency than the equilateral trenches.

According to the simulation and experimental results, the triangular trench demonstrated a reduction in local flow velocity, that would be able to enhance the trapping efficiency of microwells. Future research should focus on further improving the trench designs and developing their potential for industrial purposes and commercial applications.

In addition, further studies could investigate alternative fabrication methods and examine how the sizes of particles influence trapping efficiency.

## 6. Conclusion

In this study, we proposed the mechanism for reducing flow velocity using triangular obstacle trenches in microfluidic systems demonstrating in both simulations and experiments. This velocity reduction is achieved through two key processes. Firstly, fluid flow is directed toward the apex trench and spread out at the back of the triangular trenches. Secondly, the trench must have an appropriate depth to generate sufficient recirculation, and avoid the trapping of particles inside the trench.

To validate the simulation, the experiments were conducted by comparing equilateral, right-angle trench to a control case. The experimental results showed that the use of triangular trench increased trapping efficiency by 30 times compared to the case without trenches. However, the trapping efficiency results between both designs were comparable, with no significant differences in the number of trapped microplastics.

Ultimately, we hope this study enhances the understanding of mechanisms and key parameters for reducing local flow velocity in the obstacle trenches as well as helping readers to appropriately select parameters for higher trapping efficiency.



## 7. Acknowledgement

This work was financially supported by Thailand Toray Science Foundation. The authors would like to thank Kanit Singburana, Thatchanon Reawrunsangkul and Techin Vichainarong for the development of obstacle trench designs.

## 8. References

- [1] N.S. Roslan, Y.Y. Lee, Y.S. Ibrahim, S.T. Anuar, K.M.K.K. Yusof, L.A. Lai and T. Brentnall, Detection of microplastics in human tissues and organs: A scoping review, *Journal Of Global Health*, 2024, 14, 04179.
- [2] E. Dzierzynski, P.J. Gawlik, D. Puzniak, W. Flieger, K. Józwiak, G. Teresinski, A. Forma, P. Wdowiak, J. Baj and J. Flieger, Microplastics in the Human Body: Exposure, Detection, and Risk of Carcinogenesis: A State-of-the-Art Review, *Cancers*, 2024, 16, 3703.
- [3] F. Yu, Q. Qin, X. Zhanga and J. Ma, Characteristics and adsorption behavior of typical microplastics in long-term accelerated weathering simulation, *Environmental Science: Processes and Impacts*, 2024, 26, 882-890.
- [4] N. Rafa, B. Ahmed, F. Zohora, J. Bakya, S. Ahmed, S.F. Ahmed, M. Mofijur, A.A. Chowdhury and F. Almomani, Microplastics as carriers of toxic pollutants: Source, transport, and toxicological effects, *Environmental Pollution*, 2023, 343, 123190.
- [5] S. Abbasi, F. Moore and B. Keshavarzi, PET-microplastics as a vector for polycyclic aromatic Hydrocarbons in a simulated plant rhizosphere zone, *Environmental Technology and Innovation*, 2021, 21, 101370.
- [6] E.C. Emenike, C.J. Okorie, T. Ojeyemi, A. Egbemhenghe, K.O. Iwuozor, O.D. Saliu, H.K. Okora and A.G. Adeniyi, From oceans to dinner plates: The impact of microplastics on human health, *Heliyon*, 2023, 9, 1, e20440.
- [7] X. Chen, Z. Liang, D. Li, Y. Xiong, P. Xiong, Y. Guan, S. Hou, Y. Hu, S. Chen, G. Liu and Y. Tian, Microfluidic dielectrophoresis device for trapping, counting and detecting *Shewanella oneidensis* at the cell level, *Biosensors and Bioelectronics*, 2018, 99, 416–423.
- [8] A. Munaz, M.J.A. Shiddiky and N.T. Nguyen, Recent advances and current challenges in magnetophoresis based micro magnetofluidics, *Biomicrofluidics*, 2018, 12(3), 031501.
- [9] J.E. Molloy, K. Dholakia and M.J. Padgett, Optical tweezers in a new light, *Journal of Modern Optics*, 2003, 50(10), 1501-1507.
- [10] D. Yin, G. Xu, M. Wang, M. Shen, T. Xu, X. Zhu and X. Shi, Effective cell trapping using PDMS microspheres in an acoustofluidic chip, *Colloids and Surfaces B: Biointerfaces*, 2017, 157, 347–354.



- [11] V. Narayanamurthy, S. Nagarajan, A.Y.F. Khan, F. Samsuri and T.M. Sridhar, Microfluidic hydrodynamic trapping for single cell analysis: mechanisms, methods and application, *Analytical Methods*, 2017, 9, 3751-3772.
- [12] J.Y. Park, M. Morgan, A.N. Sachs, J. Samorezov, R. Teller, Y. Shen, K.J. Pienta and S. Takayama, Single cell trapping in larger microwells capable of supporting cell spreading and proliferation, *Microfluidics Nanofluidics*, 2010, 8(2), 263-268.
- [13] P. Yingprathanphon, T. Wongpakham, W. Srituravanich and A. Pimpin, Filling-and-Dragging Technique for particle entrapment using triangular microwell, *Engineering Journal*, 2020, 24(2), 63-74.
- [14] T. Tongmanee, W. Srituravanich, A. Sailasuta, W. Sripumkhai, W. Jeamsaksiri, K. Morimoto, Y. Suzuki and A. Pimpin, Effects of the cell and triangular microwell size on the cell-trapping efficiency and specificity, *Journal of Mechanical Science and Technology*, 2019, 33, 5571-5580.